Finite element computation of nonlinear normal modes of nonconservative systems

L. Renson[1], **G. Deliège**[2], **G. Kerschen**[1]
[1] Space Structures and Systems Laboratory (S3L), Structural Dynamics Research Group,
Department of Aerospace and Mechanical Engineering, University of Liège, Belgium.
e-mail: **l.renson@ulg.ac.be, g.kerschen@ulg.ac.be**

[2] Computational Nonlinear Mechanics,
Department of Aerospace and Mechanical Engineering, University of Liège, Belgium.
e-mail: **geoffrey.deliege@ulg.ac.be**

Abstract
Modal analysis, i.e., the computation of vibration modes of linear systems, is really quite sophisticated and advanced. Even though modal analysis served, and is still serving, the structural dynamics community for applications ranging from bridges to satellites, it is commonly accepted that nonlinearity is a frequent occurrence in engineering structures. Because modal analysis fails in the presence of nonlinear dynamical phenomena, the development of a practical nonlinear analog of modal analysis is the objective of this research. Progress in this direction has been made recently with the development of numerical techniques (harmonic balance, continuation of periodic solutions) for the computation of nonlinear normal modes (NNMs). Because these methods consider the conservative system, this study targets the computation of NNMs for nonconservative systems, i.e. defined as invariant manifolds in phase space. Specifically, a new finite element technique is proposed to solve the set of partial differential equations governing the manifold geometry. The algorithm is demonstrated using different two-degree-of-freedom systems.

1 Introduction

The dynamic systems theory is well-established for linear systems and can rely on mature tools such as the theories of linear operators and linear integral transforms. Even though linear modal analysis served, and is still serving, the structural dynamics community for applications ranging from bridges to satellites, it is commonly accepted that nonlinearity is a frequent occurrence in engineering structures [1, 2]. Because linear modal analysis fails in the presence of nonlinear dynamical phenomena, the development of a practical nonlinear analog of modal analysis is a problem of great timeliness and importance.

Nonlinear normal modes (NNMs), which are a rigorous extension of the linear normal modes (LNMs) to nonlinear systems, were pioneered in the 1960s by Rosenberg [3, 4]. He defined an NNM as a *vibration in unison* of the system. Shaw and Pierre proposed a generalization of Rosenberg's definition that provides an elegant extension of the NNM concept to damped systems. Based on geometric arguments and inspired by the center manifold theory, they defined an NNM as a two-dimensional invariant manifold in phase space [5, 6].

If a large body of literature has addressed the computation of NNMs using analytical techniques (see, e.g., [6, 7, 8, 9, 10]), there have been relatively few attempts to compute NNMs using numerical methods. Most of these latter methods compute undamped NNMs, which are considered as periodic solutions of the underlying Hamiltonian system [11, 12, 13, 14, 15]. On the one hand, this is particularly attractive when targeting

a numerical computation of the NNMs; it paves the way for the application of the NNM theory to large-scale, complex structures [16]. On the other hand, the influence of (linear and nonlinear) damping cannot be studied, which may be an important limitation in practice.

The first attempt to carry out numerical computation of damped NNMs is that of Pesheck et al. [17, 18]. The manifold-governing partial differential equations (PDEs) are solved in modal space using a Galerkin projection with the NNM motion parametrized by amplitude and phase variables. This method eliminates a number of problems associated with the local polynomial approximation of the manifold [6]. Probably the most significant advantage is that the computation of NNMs in large-amplitude regimes can be handled. In a recent contribution, Touz and co-workers [19] also tackle the PDEs in modal space. They show that these PDEs can be interpreted as a transport equation, which, in turn, can be discretized using finite differences. In the study by Noreland et al. [20], the manifold is described by partial differential algebraic equations, which are also solved by finite differences. Another interesting approach uses a Fourier-Galerkin procedure and relies on the concept of complex nonlinear modes [21]. It does not solve the governing equations of the manifold, but it is able to compute it *a posteriori*.

The present study introduces a new method for the numerical computation of NNMs defined as invariant manifolds in phase space. The transformation of the manifold-governing PDEs to modal space is not necessary, which means that an NNM motion is parametrized by master displacement and velocity, as in [6]. We propose to solve the set of PDEs using the finite element (FE) method, which renders the method general and systematic.

The paper is organized as follows. In Section 2, a brief review of NNMs is achieved, and the manifold-governing PDEs are introduced. Section 3 describes how the FE method can be exploited for the computation of undamped and damped NNMs. In Section 4, the proposed algorithm is demonstrated using three examples, namely a damped linear system, an undamped nonlinear system, and a damped nonlinear system, all possessing two degrees of freedom. The conclusions of the present study are summarized in Section 5.

2 Review of normal modes for nonlinear systems

2.1 Definitions

A detailed description of NNMs and of their fundamental properties (e.g., frequency-energy dependence, bifurcations, and stability) is given in [9, 22] and is beyond the scope of this paper. For completeness, the two main definitions of an NNM are briefly reviewed in this section.

The free response of discrete mechanical systems with N degrees of freedom (DOFs) is considered, assuming that continuous systems (e.g., beams, shells, or plates) have been spatially discretized using the FE method. The equations of motion are

$$\mathbf{M}\,\ddot{\mathbf{x}}(t) + \mathbf{C}\,\dot{\mathbf{x}}(t) + \mathbf{K}\,\mathbf{x}(t) + \mathbf{f}_{\text{nl}}\left\{\mathbf{x}(t), \dot{\mathbf{x}}(t)\right\} = 0 \tag{1}$$

where $\mathbf{M}$, $\mathbf{C}$, and $\mathbf{K}$ are the mass, damping, and stiffness matrices, respectively; $\mathbf{x}$, $\dot{\mathbf{x}}$, and $\ddot{\mathbf{x}}$ are the displacement, velocity, and acceleration vectors, respectively; $\mathbf{f}_{\text{nl}}$ is the nonlinear restoring force vector.

Targeting a straightforward nonlinear extension of the concept of LNMs, Rosenberg defined an NNM motion as a synchronous periodic oscillation. This definition requires that all material points of the system reach their extreme values and pass through zero simultaneously and allows all displacements to be expressed in terms of a single reference displacement. At first glance, Rosenberg's definition may appear restrictive in two cases:

1. In the presence of internal resonances, an NNM motion is no longer synchronous, but it is still periodic. This is why an extended definition was considered in [12, 22]; an NNM motion was defined as a *(non-necessarily synchronous) periodic motion* of the undamped mechanical system.

2. The definition cannot be easily extended to nonconservative systems. However, as shown in [22], the damped dynamics can be interpreted based on the topological structure of the NNMs of the underlying conservative system, provided that damping has a purely parasitic effect.

For illustration, the system depicted in Figure 1 and governed by the equations

$$\begin{aligned} \ddot{x}_1 + (2x_1 - x_2) + 0.5\,x_1^3 &= 0 \\ \ddot{x}_2 + (2x_2 - x_1) &= 0 \end{aligned} \tag{2}$$

is considered. The NNMs corresponding to in-phase and out-of-phase motions are represented in the frequency-energy plot (FEP) of Figure 2. An NNM is represented by a point in the FEP, which is drawn at a frequency corresponding to the minimal period of the periodic motion and at an energy equal to the conserved total energy during the motion. A branch, represented by a solid line, is a family of NNM motions possessing the same qualitative features (e.g., in-phase NNM motion).

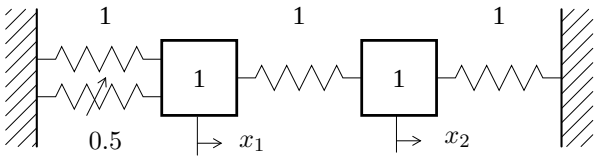

Figure 1: Schematic representation of the 2DOF system example.

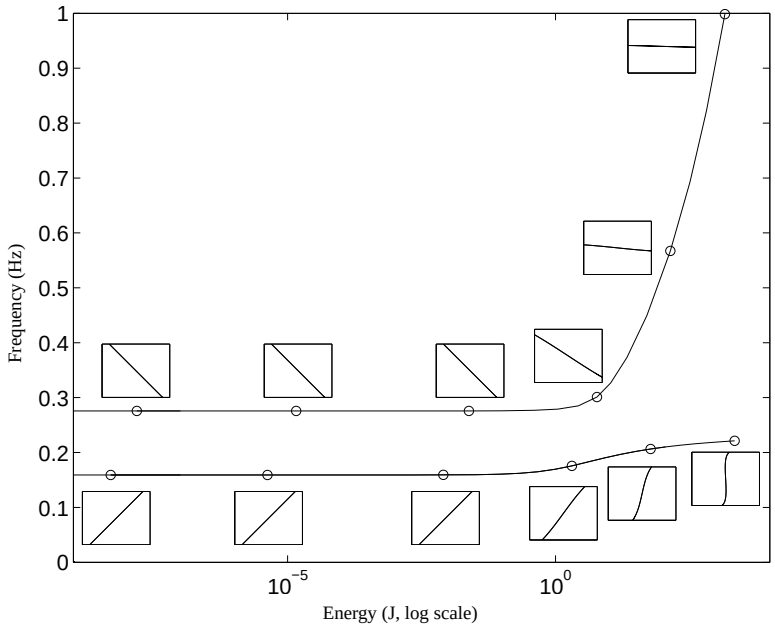

Figure 2: Frequency-energy plot of system (2). NNM motions depicted in the configuration space are inset.

To provide a rigorous extension of the NNM concept to damped systems, Shaw and Pierre defined an NNM as a two-dimensional invariant manifold in phase space. Such a manifold is invariant under the flow (i.e., orbits that start out in the manifold remain in it for all time), which generalizes the invariance property of LNMs to nonlinear systems. In order to parametrize the manifold, a single pair of state variables (i.e., both the displacement and the velocity) are chosen as master coordinates, the remaining variables being functionally related to the chosen pair. Therefore, the system behaves like a nonlinear single-DOF system on the manifold.

Geometrically, LNMs are represented by planes in phase space, and NNMs are two-dimensional surfaces that are tangent to them at the equilibrium point. The invariant manifolds corresponding to in-phase and out-of-phase NNM motions of system (2) are given in Figure 3.

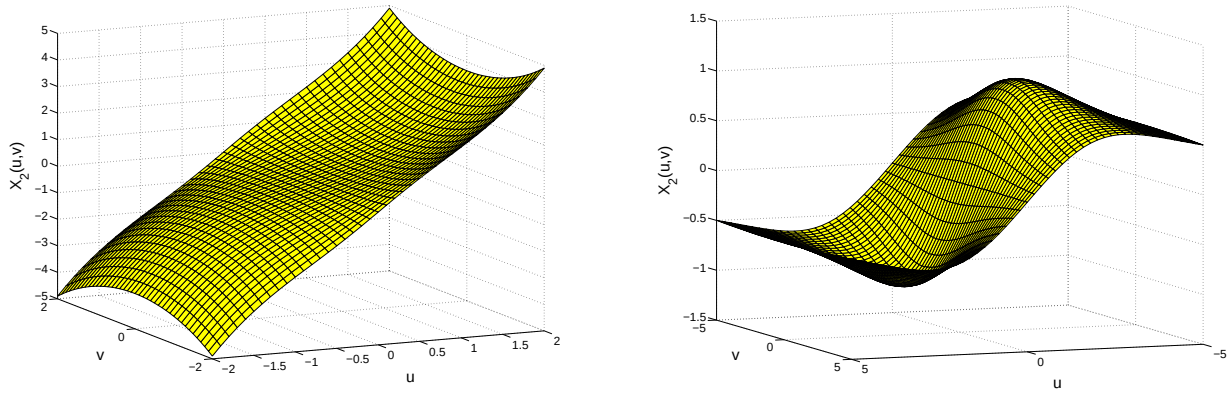

(a) (b)

Figure 3: Two-dimensional invariant manifolds of system (2) computed with an algorithm for the continuation of periodic solutions. (a) In-phase NNM; and (b) out-of-phase NNM.

2.2 Manifold-governing partial differential equations

To derive the equations governing the geometry of the manifold, Equations (1) are recast into state-space form:

$$\begin{aligned} \dot{x}_i &= y_i, \\ \dot{y}_i &= f_i(\mathbf{x}, \mathbf{y}), \qquad i = 1, ..., N. \end{aligned} \tag{3}$$

The formulation and notations presented here closely follow those used in reference [6].

During an NNM motion, there is a functional dependence between all degrees of freedom, and the motion can be parametrized by a single displacement-velocity pair. The selection of the master coordinates $(u, v) = (x_k, y_k)$, i.e., the nonlinear modal coordinates, is arbitrary. The $2N - 2$ constraint equations governing the slave coordinates are:

$$\begin{aligned} x_i &= X_i(u, v), \\ y_i &= Y_i(u, v) \qquad i = 1, ..., N;\ i \neq k. \end{aligned} \tag{4}$$

To obtain a set of equations governing the manifold geometry, i.e., the X_i's and Y_i's, the time dependence in the equations is eliminated. Taking the time derivative of the constraint equations (4) and using the chain rule for differentiation yields:

$$\begin{aligned} \dot{x}_i &= \frac{\partial X_i}{\partial u}\dot{u} + \frac{\partial X_i}{\partial v}\dot{v} \\ \dot{y}_i &= \frac{\partial Y_i}{\partial u}\dot{u} + \frac{\partial Y_i}{\partial v}\dot{v}, \qquad i = 1, ..., N;\ i \neq k. \end{aligned} \tag{5}$$

Plugging Equations (3) and (4) into Equation (5) leads to a set of $2N-2$ partial differential equations (PDEs) that can be solved for the X_i's and Y_i's:

$$\begin{aligned} Y_i(u, v) &= \frac{\partial X_i(u, v)}{\partial u} v + \frac{\partial X_i(u, v)}{\partial v} f_k(u, \mathbf{X}(u, v), v, \mathbf{Y}(u, v)) \\ f_i(u, \mathbf{X}(u, v), v, \mathbf{Y}(u, v)) &= \frac{\partial Y_i(u, v)}{\partial u} v + \frac{\partial Y_i(u, v)}{\partial v} f_k(u, \mathbf{X}(u, v), v, \mathbf{Y}(u, v)) \\ & \qquad i = 1, ..., N;\ i \neq k, \end{aligned} \tag{6}$$

where $\mathbf{X} = \{X_j : j = 1, ..., N\ ; j \neq k\}$ and $\mathbf{Y} = \{Y_j : j = 1, ..., N\ ; j \neq k\}$. Equations for $i = k$ are trivially satisfied.

Once the manifold-governing PDEs are solved, constraint equations (4) represent the geometrical description of the NNM. Equations (6) admit N solutions, i.e., one for each mode. The nonlinear modal dynamics is then generated by substituting the X_i's and Y_i's in the pair of equations of motion governing the master coordinates x_k and y_k. This results in a single-DOF nonlinear motion:

$$\begin{aligned} \dot{u} &= v, \\ \dot{v} &= f_k(u, \mathbf{X}(u,v), v, \mathbf{Y}(u,v)), \qquad i = 1, ..., N;\ i \neq k. \end{aligned} \tag{7}$$

3 Finite element computation of nonlinear normal modes

The set of PDEs (6) is as difficult to solve as the original problem, but the solution can be approximated using power series, as reported in reference [6]. Such an analytical approach has the advantage that NNMs can be constructed symbolically. However, the resultant dynamics are only accurate for small-amplitude motions, and the upper bound for these motions is not known a priori.

To address these limitations, we propose to solve the equations governing the manifold numerically using the FE method. To this end, a weak form of these equations is obtained using the Galerkin weighted residual approach [23]. By integrating the residue of the PDEs multiplied by the appropriate virtual fields δX_i and δY_i to preserve unit consistency, Equations (6) become:

$$\begin{aligned} \iint_\Omega \left[Y_i(u,v) - \frac{\partial X_i(u,v)}{\partial u} v - \frac{\partial X_i(u,v)}{\partial v} f_k(u,v,\mathbf{X},\mathbf{Y}) \right] \delta Y_i \, \mathrm{d}u\mathrm{d}v = 0 \\ \iint_\Omega \left[f_i(u,v,\mathbf{X},\mathbf{Y}) - \frac{\partial Y_i(u,v)}{\partial u} v - \frac{\partial Y_i(u,v)}{\partial v} f_k(u,v,\mathbf{X},\mathbf{Y}) \right] \delta X_i \, \mathrm{d}u\mathrm{d}v = 0 \end{aligned} \tag{8}$$

where $i = 1, ..., N$ and $i \neq k$. The domain Ω is defined *a priori* as

$$\Omega = \left\{ (u,v) \in \Re^2 : u_{\min} < u < u_{\max}, v_{\min} < v < v_{\max} \right\} \tag{9}$$

and is decomposed into FEs. The unknown and virtual fields within an element e are expressed in terms of the nodal values $X_i^a, Y_i^a, \delta X_i^b$ and δY_i^b, shape functions $N^a(u,v)$ and test functions $N^b(u,v)$. In the present study, linear rectangular FEs with 4 nodes ($n = 4$) are considered. The shape functions are $N^a(u,v) = \frac{1}{4}(1 + u_a u)(1 + v_a v)$ with u_a and v_a the values of the coordinates at node a. The same expressions are used for test functions.

The integral over the domain Ω in Equations (8) is evaluated by summing the integral obtained over each of the elements which pave the domain. This yields:

$$\begin{aligned} \sum_e \iint_{\Omega_e} \left[\sum_a N^a Y_i^{e,a} - \sum_a \frac{\partial N^a}{\partial u} X_i^{e,a} v - \sum_a \frac{\partial N^a}{\partial v} X_i^{e,a} f_k^e \right] \sum_b N^b \delta Y_i^{e,b} \, \mathrm{d}u\mathrm{d}v = 0 \\ \sum_e \iint_{\Omega_e} \left[f_i^e - \sum_a \frac{\partial N^a}{\partial u} Y_i^{e,a} v - \sum_a \frac{\partial N^a}{\partial v} Y_i^{e,a} f_k^e \right] \sum_b N^b \delta X_i^{e,b} \, \mathrm{d}u\mathrm{d}v = 0 \end{aligned} \tag{10}$$

where, for conciseness, $f_{k,i}^e = f_{k,i}(u, v, \mathbf{X}^e, \mathbf{Y}^e)$.

For convenience, a mapping from elements in global coordinates to a reference element with local normalized coordinates (ξ,η) is considered (Equations (11)). Variables u and v are replaced by the mapping whereas the derivatives with respect to these variables are transformed using the chain rule.

$$\left\{ \begin{array}{c} u \\ v \end{array} \right\} = \left\{ \begin{array}{c} g_u(\xi,\eta) \\ g_v(\xi,\eta) \end{array} \right\} \tag{11}$$

The set of $2N-2$ equations discretized by the FE method (10) has to be satisfied for arbitrary virtual fields $\delta X_i^{e,b}$ and $\delta Y_i^{e,b}$. This leads to a new set of equations for which the number of unknowns equals the number of equations (i.e., $2n(N-1)$ per element):

$$\mathscr{L}(\mathbf{Z}) = \sum_e \left\{ \underbrace{\begin{pmatrix} -\mathbf{M}_2^e & \mathbf{M}_1^e \\ \mathbf{0} & -\mathbf{M}_2^e \end{pmatrix}}_{2n(N-1)\times 2n(N-1)} \underbrace{\mathbf{Z}^e}_{2n(N-1)\times 1} + \underbrace{\begin{pmatrix} -\mathbf{F}_1^e(\mathbf{Z}^e) \\ \mathbf{F}_2^e(\mathbf{Z}^e) - \mathbf{F}_3^e(\mathbf{Z}^e) \end{pmatrix}}_{2n(N-1)\times 1} \right\} = \mathbf{0} \tag{12}$$

where $\mathbf{Z}^e$ contains the nodal values of the considered FE:

$$\mathbf{Z}^e = \begin{bmatrix} X_2^{e,a} & \dots & X_N^{e,a} & Y_2^{e,a} & \dots & Y_N^{e,a} \end{bmatrix}^{\mathrm{T}} \tag{13}$$

Vector $\mathbf{Z}$ is the proper assembly of all vectors $\mathbf{Z}^e$; it therefore contains all nodal unknowns. Matrices $\mathbf{M}_1^e$, $\mathbf{M}_2^e$ and vectors $\mathbf{F}_1^e$, $\mathbf{F}_2^e$, and $\mathbf{F}_3^e$ are defined as the block-assembly of $\mathbf{M}_{1i}^e$, $\mathbf{M}_{2i}^e$, $\mathbf{F}_{1i}^e$, $\mathbf{F}_{2i}^e$, and $\mathbf{F}_{3i}^e$ ($i = 1, ..., N;\ i \neq k$), respectively. $\mathbf{M}_{1i}^e$ and $\mathbf{M}_{2i}^e$ are $n \times n$ matrices, and $\mathbf{F}_{1i}^e$, $\mathbf{F}_{2i}^e$, and $\mathbf{F}_{3i}^e$ are $n \times 1$ vectors. The $\mathbf{F}_i^e$'s are the nonlinear forces acting on the system.

The elements of these matrices and vectors are defined as:

$$\begin{aligned}
M_{1i}^{e,ba} &= \int_{-1}^{+1}\int_{-1}^{+1} N^a N^b \det(\mathbf{J}) \mathrm{d}\xi \mathrm{d}\eta, \\
M_{2i}^{e,ba} &= \int_{-1}^{+1}\int_{-1}^{+1} \left(\frac{\partial g_v}{\partial \eta}\frac{\partial N^a}{\partial \xi} - \frac{\partial g_v}{\partial \xi}\frac{\partial N^a}{\partial \eta} \right) g_v N^b \mathrm{d}\xi \mathrm{d}\eta, \\
F_{1i}^{e,b} &= \int_{-1}^{+1}\int_{-1}^{+1} \sum_a \left(\frac{\partial g_u}{\partial \xi}\frac{\partial N^a}{\partial \eta} - \frac{\partial g_u}{\partial \eta}\frac{\partial N^a}{\partial \xi} \right) X_i^{e,a} f_k^e N^b \mathrm{d}\xi \mathrm{d}\eta, \\
F_{2i}^{e,b} &= \int_{-1}^{+1}\int_{-1}^{+1} f_i^e N^b \det(\mathbf{J}) \mathrm{d}\xi \mathrm{d}\eta, \\
F_{3i}^{e,b} &= \int_{-1}^{+1}\int_{-1}^{+1} \sum_a \left(\frac{\partial g_u}{\partial \xi}\frac{\partial N^a}{\partial \eta} - \frac{\partial g_u}{\partial \eta}\frac{\partial N^a}{\partial \xi} \right) Y_i^{e,a} f_k^e N^b \mathrm{d}\xi \mathrm{d}\eta.
\end{aligned} \tag{14}$$

$\mathbf{J}$ is the Jacobian matrix of the mapping. Two types of boundary conditions are considered. They arise directly from the definition of an NNM as an invariant manifold in phase space:

1. The manifold passes through the equilibrium point. Without loss of generality, it is considered at $(u, v) = (0, 0)$, and $X_i(0, 0) = Y_i(0, 0) = 0$ with $i = 1, ..., N;\ i \neq k$.

2. At the equilibrium point, the surface defined by the manifold must be tangent to the plane defined by the mode of the underlying linear system. This condition is important, because it specifies which solution out of the N different solutions is sought. The constraint is imposed on the slope of the elements around the origin.

Finally, nonlinear equations (12) are solved for the unknown vector $\mathbf{Z}$ using a classical Newton-Raphson resolution scheme.

4 Numerical Examples

In this section, the demonstration of the new numerical procedure for NNM computation is carried out using the two-DOF system in Figure 1. The linear nonconservative is first considered, and the nonlinear system (both conservative and nonconservative cases) is tackled next.

4.1 Linear nonconservative system

Nonproportional damping is added to Equations (2), and the nonlinearity is ignored to yield:

$$\begin{aligned} \ddot{x}_1 + 0.3(\dot{x}_1 - \dot{x}_2) + (2x_1 - x_2) &= 0 \\ \ddot{x}_2 + (0.6\dot{x}_2 - 0.3\dot{x}_1) + (2x_2 - x_1) &= 0 \end{aligned} \tag{15}$$

In this case, the solution is easily obtained by the algorithm, because the first guess $\mathbf{Z}^0$ in the Newton-Raphson scheme coincides with the LNM.

Nonetheless, this example offers a means of validating the developed algorithm, as the residue $||\mathscr{L}(\mathbf{Z})||_2$ is effectively zero ($\approx 10^{-16}$) when either the in-phase or out-of-phase LNM are inserted into Equations (12).

4.2 Nonlinear conservative system

For conservative system (2), the "exact" manifolds can be computed using the technique developed in [15], which combines shooting and pseudo-arclength continuation. For both the in-phase and out-of-phase NNMs, the graphical depiction in phase space of the periodic orbits at different energy levels provides a reference solution. For comparison purposes, the manifold computed using Shaw and Pierre power series expansion [6] is also represented. The expansion is carried out at third and fifth orders.

Considering the domain $\Omega_1 = \left\{(u,v) \in \Re^2 : -1 < u < 1, -1 < v < 1\right\}$ and starting from the in-phase LNM, convergence of the FE algorithm is obtained after 6 iterations ($||\mathscr{L}(\mathbf{Z})||_2 \approx 10^{-16}$). Figure 4 presents a comparison of the in-phase invariant manifold obtained with the three techniques (i.e., reference, SP3, FE). Both X_2 and Y_2 are depicted in Figures 4 (a) and (b), respectively. Clearly, the analytical and numerical methods provide results that are in close agreement with the reference solution. Carrying out the power series expansion at order 5 further increases the accuracy of the analytic method, as displayed in Figures 5 (a,b).

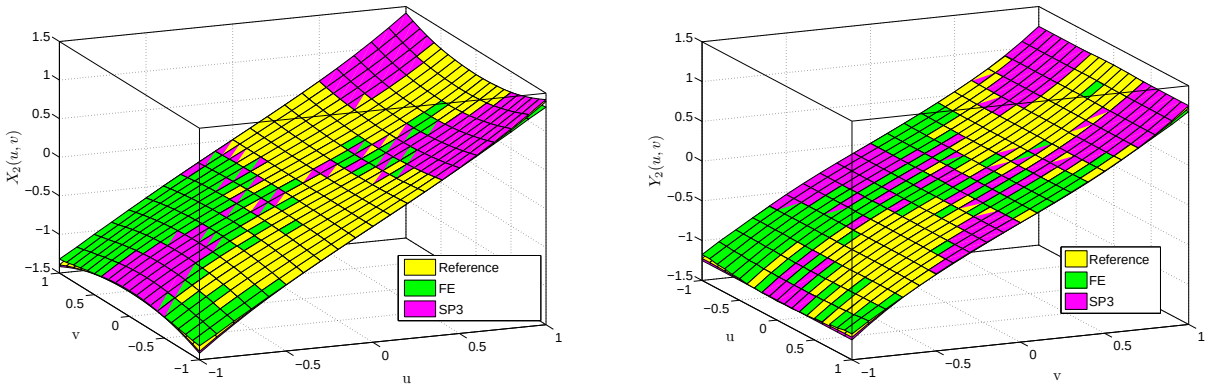

(a) (b)

Figure 4: Invariant manifold of the in-phase mode of the nonlinear conservative system in Ω_1. The manifold is computed using shooting and pseudo-arclength continuation (reference), Shaw and Pierre power series expansion at order 3 (SP3) and the FE method. (a) X_2; and (b) Y_2.

For a larger computation domain, i.e., $\Omega_2 = \left\{(u,v) \in \Re^2 : 2 < u < 2, -2 < v < 2\right\}$, Figure 6 shows that the FE method continues to provide accurate results, whereas the analytic method does no longer agree with the reference solution. Interestingly, expanding the solution at order 5 does not improve the results, at least at the domain boundaries (see Figure 7). This observation highlights one important limitation of the asymptotic approach; i.e, the convergence domain of the expansion is unknown *a priori*.

A more quantitative comparison of the results is now carried out. The initial conditions in the modal space (u,v) of the in-phase mode computed through the FE method are transformed back to physical space

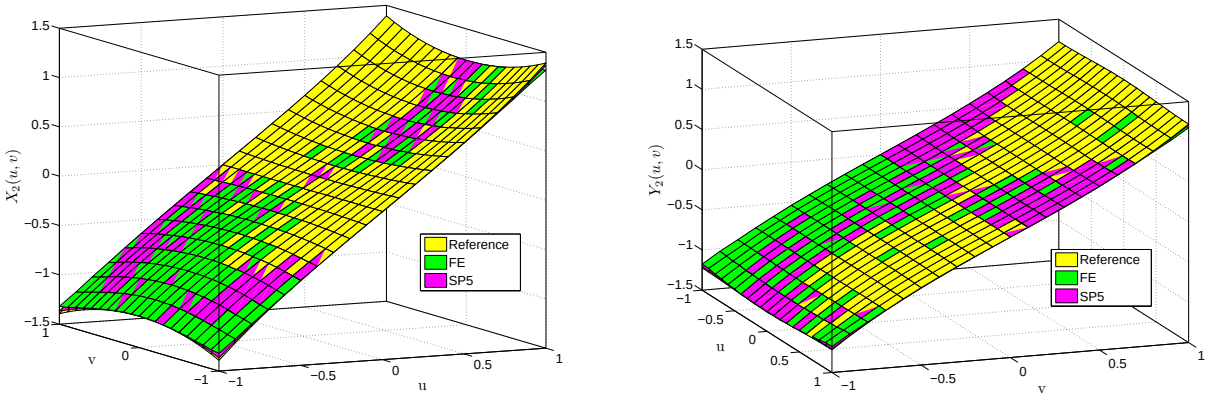

(a) (b)

Figure 5: Invariant manifold of the in-phase mode of the nonlinear conservative system in Ω_1. The manifold is computed using shooting and pseudo-arclength continuation (reference), Shaw and Pierre power series expansion at order 5 (SP5) and the FE method. (a) X_2; and (b) Y_2.

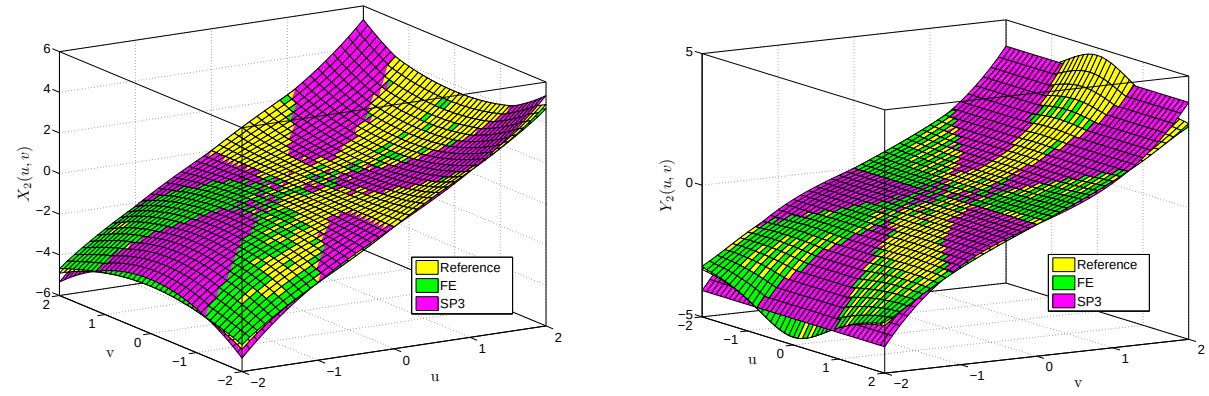

(a) (b)

Figure 6: Invariant manifold of the in-phase mode of the nonlinear conservative system in Ω_2. The manifold is computed using shooting and pseudo-arclength continuation (reference), Shaw and Pierre power series expansion at order 3 (SP3) and the FE method. (a) X_2; and (b) Y_2.

(x_1, y_1, x_2, y_2) using Equation (4). Both the equations of motion in physical space (2) and in modal space (7) are numerically integrated for these initial conditions using Runge-Kutta method. The resulting time series in modal space are then transformed back to physical space and compared to the time series generated directly in physical space. The comparison is achieved using the normalized mean-square error (NMSE):

$$\text{NMSE}(\hat{f}) = \frac{100}{N\sigma_f^2} \sum_{i=1}^{N} (f(i) - \hat{f}(i))^2 \tag{16}$$

where $\hat{f}$ is the time series to be compared to the reference series f, N is the number of samples and σ_f^2 is the variance of the reference time series. A NMSE value of 1% is commonly assumed to reflect excellent concordance between the time series. Table 1 lists the results for the different methods and two sets of initial conditions corresponding to medium- and high-energy in-phase mode motions. At medium energy, the asymptotic method accuracy does not exceed 0.1%. The fifth-order expansion provides better results than the third-order expansion but it is less accurate than the FE method. At high energy, the FE method is still accurate, whereas the solution provided by the analytic method can no longer be trusted. The third-order expansion is now more accurate than the fifth-order solution, which confirms the graphical observation in

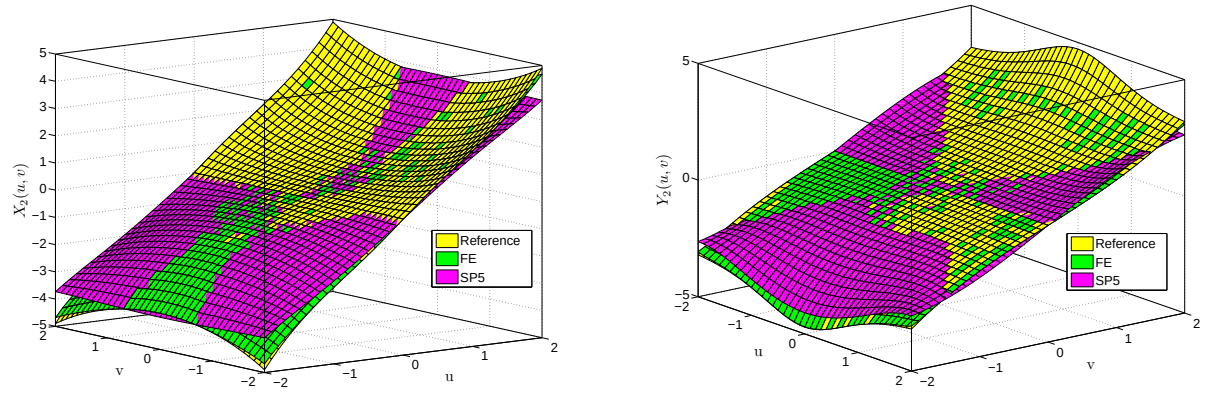

(a) (b)

Figure 7: Invariant manifold of the in-phase mode of the nonlinear conservative system in Ω_2. The manifold is computed using shooting and pseudo-arclength continuation (reference), Shaw and Pierre power series expansion at order 5 (SP5) and the FE method. (a) X_2; and (b) Y_2.

Figure 7.

Initial conditions: $w = [0.95\ 0]$			
	SP 3[rd] order	SP 5[th] order	FE method
NMSE$_u$	0.06	0.03	10^{-3}
NMSE$_v$	0.07	0.03	10^{-3}
NMSE$_{X_2}$	0.06	0.03	10^{-3}
NMSE$_{Y_2}$	0.07	0.03	10^{-3}
Initial conditions: $w = [1.95\ 0]$			
NMSE$_u$	9.3	52.8	10^{-2}
NMSE$_v$	11.2	62.1	10^{-2}
NMSE$_{X_2}$	9.6	50.0	10^{-2}
NMSE$_{Y_2}$	9.7	54.0	10^{-2}

Table 1: NMSE obtained using the different methods for medium- and high-energy in-phase mode motions of the nonlinear conservative system.

Considering now the out-of-phase NNM in Ω_1, Figure 8 depicts that the FE method is associated with nonnegligible error, which amounts to 22 % at the corners of the domain. Conversely, the asymptotic method provides an excellent approximation of the invariant manifold. Considering the larger domain Ω_2 confirms the inability of the FE method to retrieve the reference results (see Figure 9). Even though Figure 10 shows that the fifth-order approximation gives rise to some improvement, the analytic method is also unable to compute the out-of-phase NNM accurately in Ω_2.

The failure of the FE method in the particular case of the out-of-phase NNM can be explained by recognizing that the manifold-governing PDEs can be recast in the form of Equations (17) and are quasilinear hyperbolic equations where $\mathbf{V} = [v\ f_k]^{\mathrm{T}}$ represents the flow velocity. We note that this interpretation is consistent with the observation of Touzé et al. [19]. They viewed the same PDEs, but in modal space, as a transport equation with nonlinear source terms. Here, the flow corresponds to the dynamics of the master coordinates.

$$\begin{aligned} \mathbf{V}^{\mathrm{T}} \cdot \nabla X_i - Y_i &= 0 \\ \mathbf{V}^{\mathrm{T}} \cdot \nabla Y_i - f_i &= 0 \end{aligned} \tag{17}$$

It is well known that solving hyperbolic PDEs requires boundary conditions where the velocity vector points

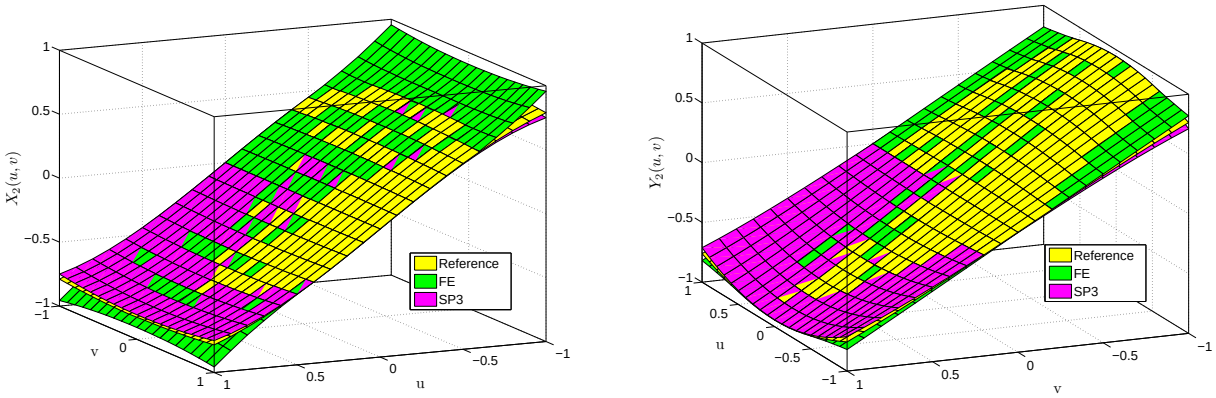

(a) (b)

Figure 8: Invariant manifold of the out-of-phase mode of the nonlinear conservative system in Ω_1. The manifold is computed using shooting and pseudo-arclength continuation (reference), Shaw and Pierre power series expansion at order 3 (SP3) and the FE method. (a) X_2; and (b) Y_2.

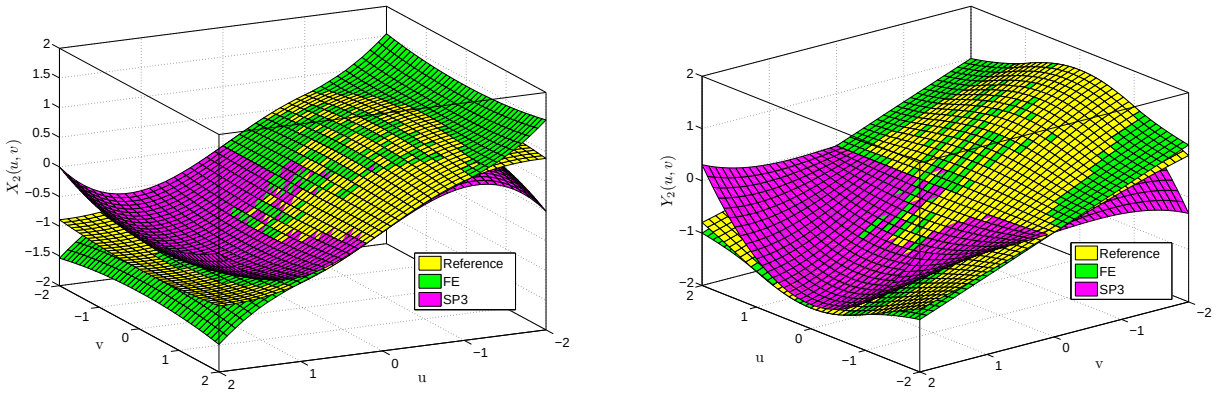

(a) (b)

Figure 9: Invariant manifold of the out-of-phase mode of the nonlinear conservative system in Ω_2. The manifold is computed using shooting and pseudo-arclength continuation (reference), Shaw and Pierre power series expansion at order 3 (SP3) and the FE method. (a) X_2; and (b) Y_2.

inward the domain (inflow). For illustration, Figure 11 presents the velocity field and an iso-energy curve for the in-phase and out-of-phase NNMs. Since the conservative system is considered, the velocity field is everywhere tangent to iso-energy curves. Because the domain approximates well the iso-energy curves of the in-phase NNM, boundary conditions are artificially fulfilled, and the computation of this mode using the FE method is much more accurate. It also explains why the largest error occurs at the corner of the domain (see, e.g, Figure 6). Further evidence of this finding is given in Figure 12 where the out-of-phase NNM is computed in the rectangular domain $\Omega_3 = \left\{(u,v) \in \Re^2 : -2 < u < 2, -5 < v < 5\right\}$, the shape of which is in much better agreement with that of the iso-energy curve compared to Ω_2. Despite that a larger domain is now considered, there is an almost perfect agreement between the reference solution and the manifold computed through the FE method. It also becomes clear that iso-energy curves are in fact the characteristic curves of the hyperbolic PDEs. Using the characteristic theory [24] to interpret Figure 11 shows that low- and high-energy dynamics do not influence each other. Indeed the information is only transported along the characteristic (i.e. iso-energy) curves creating a clear separation between different energy dynamics.

In addition to domain reshaping, another remedy proposed in the technical literature is to add supplementary boundary conditions where the velocity vector points inward (inflow) the domain. In practice, this option is

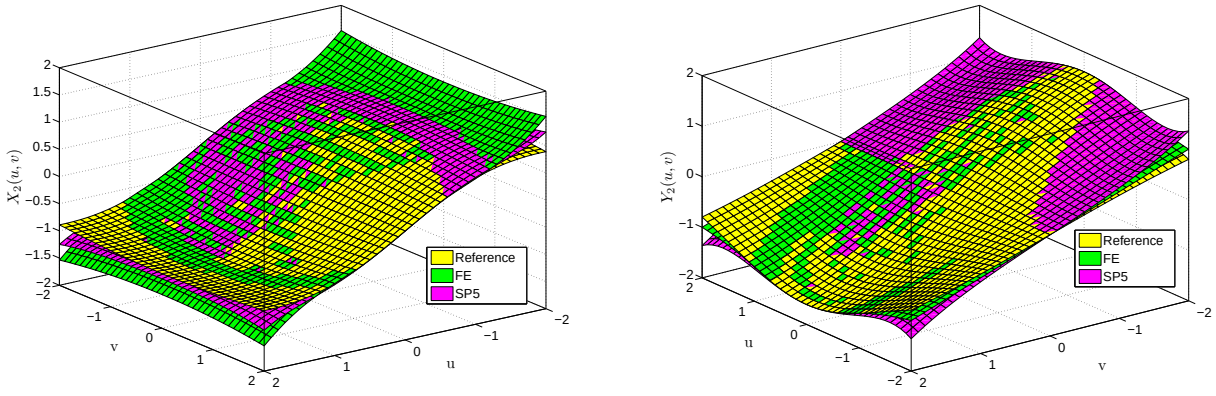

(a) (b)

Figure 10: Invariant manifold of the out-of-phase mode of the nonlinear conservative system in Ω_2. The manifold is computed using shooting and pseudo-arclength continuation (reference), Shaw and Pierre power series expansion at order 5 (SP5) and the FE method. (a) X_2; and (b) Y_2.

not further considered in order to avoid potential mixing between dynamics of different energies.

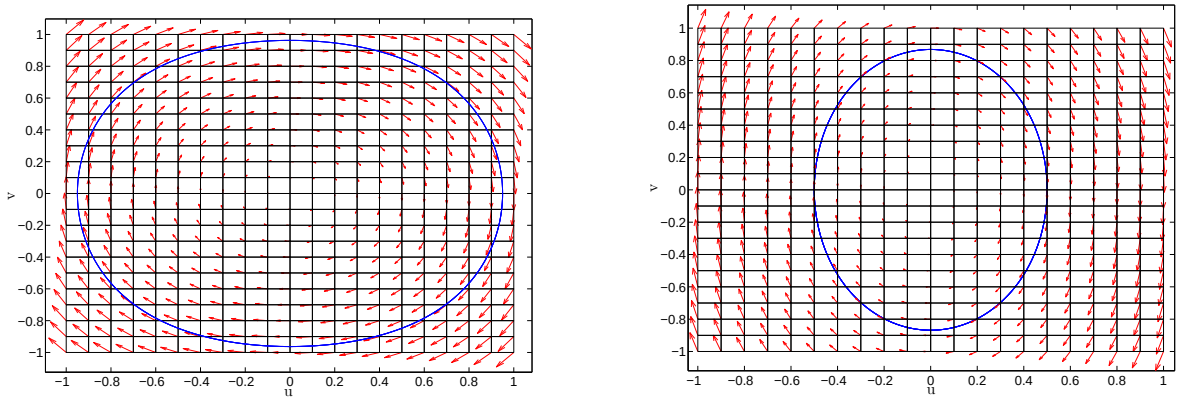

(a) (b)

Figure 11: Velocity vector ($\rightarrow$) and iso-energy curve ($-$) in the domain Ω_1. (a) In-phase NNM; and (b) out-of-phase NNM.

The study presented in this section highlights that the manifold-governing PDEs have a hyperbolic nature, which requires special treatment. Reshaping the domain therefore seems an interesting step toward the computation of high-accuracy invariant manifolds. One limitation is that this requires the knowledge of the iso-energy curves. However, thanks to the observation of characteristics, an algorithm starting from a small domain around the origin and using progressive annular domain resolution can be developed, paving the way for automatic domain adjustment. This strategy is interesting as it would reduce the computational burden for higher dimensional systems. Further research will also consider advanced finite elements methods that are widely used in fluid dynamics for solving hyperbolic PDEs (e.g., streamline upwind Petrov-Galerkin (SUPG) [25], Galerkin/Least-Squares (GLS) [25], and discontinuous Galerkin (DG) [26]).

4.3 Nonlinear nonconservative system

For the nonconservative version of system (2) with linear nonproportional damping as in (15), the ”exact” manifolds cannot be computed. Therefore, the assessment of the results is carried out through reconstruction

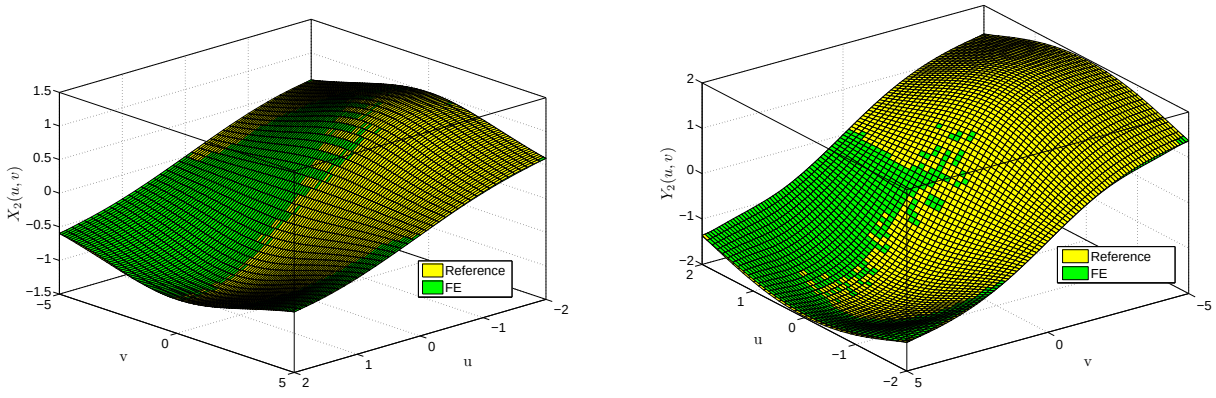

(a) (b)

Figure 12: Invariant manifold of the out-of-phase mode of the nonlinear conservative system in the rectangular domain Ω_3. The maximum relative error appears at the corners and does not exceed 6%.

of the dynamics as in Section 4.2. The methodology is similar to the one presented for the conservative system. The NMSE is again used.

Considering the domain Ω_2, Figures 13 and 14 present the manifold computed for the in-phase and out-of-phase NNMs, respectively. Table 2 lists the NMSE for the different methods medium- and high-energy in-phase mode motions. For medium energies, all methods provide accurate results with an error that does not exceed 0.01%. However, as in the conservative case, the accuracy of the asymptotic method drops while the FE method preserves its accuracy. At high energy, the FE method is still accurate, whereas the error of the analytic solution reaches 1%. Contrary to the conservative case, the fifth order expansion is now more accurate than the third-order solution.

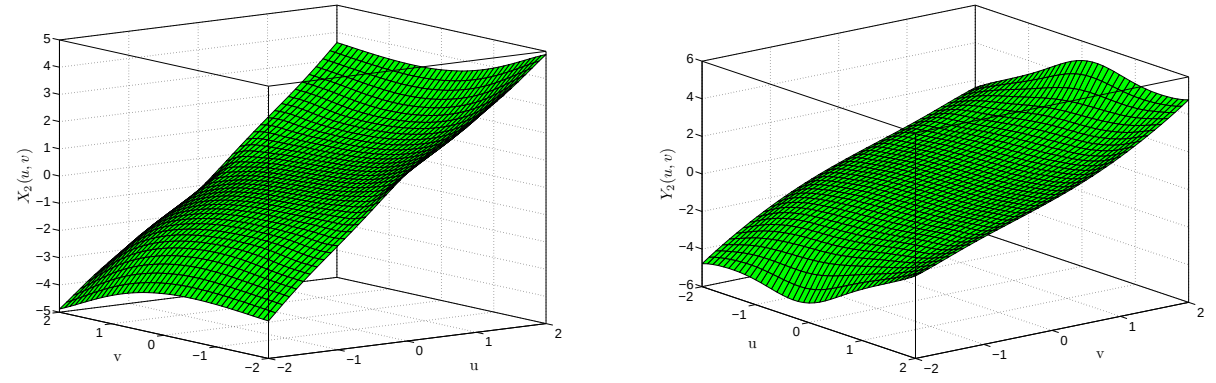

(a) (b)

Figure 13: Invariant manifold of the in-phase mode of the nonlinear nonconservative system in Ω_2. The manifold is computed using the FE method. (a) X_2; and (b) Y_2.

Linear damping therefore seems to improve the quality of the dynamics resulting from the asymptotic method. The NMSE values have decreased with respect to the conservative results. However, linear damping has no influence on the FE method, which presents the same accuracy as in the conservative case. The accuracy of the FE method also appears to remain constant over the computational domain.

Investigations on the out-of-phase mode reveal that accurate results with NMSE values lower than 0.01% are obtained despite the selection of Ω_2 as computational domain.

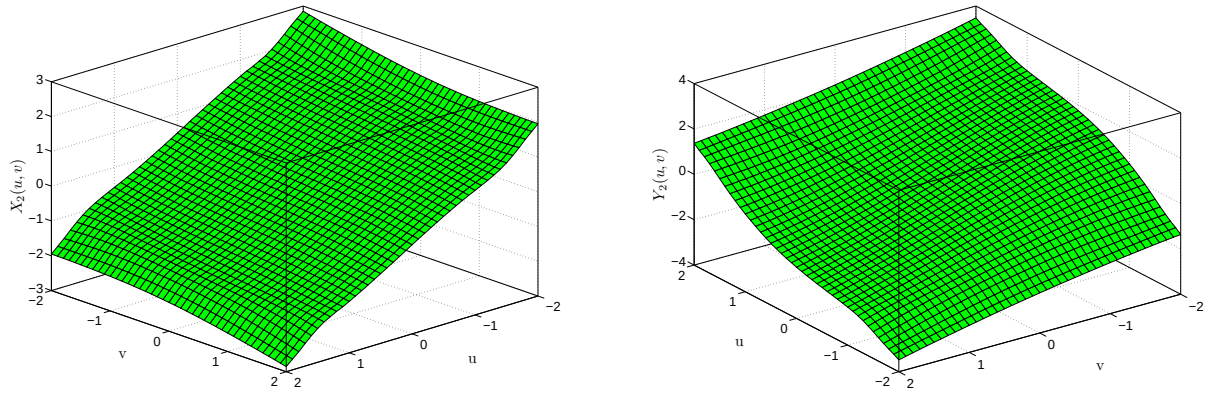

(a) (b)

Figure 14: Invariant manifold of the out-of-phase mode of the nonlinear nonconservative system in Ω_2. The manifold is computed using the FE method. (a) X_2; and (b) Y_2.

Initial conditions: $w = [0.95\ 0]$			
	SP 3^{rd} order	SP 5^{th} order	FE method
NMSE_u	10^{-2}	10^{-4}	10^{-3}
NMSE_v	10^{-2}	10^{-4}	10^{-3}
NMSE_{X_2}	10^{-2}	10^{-4}	10^{-3}
NMSE_{Y_2}	10^{-2}	10^{-3}	10^{-3}
Initial conditions: $w = [1.95\ 0]$			
NMSE_u	1.8	0.6	10^{-2}
NMSE_v	1.9	0.8	10^{-2}
NMSE_{X_2}	1.8	0.9	10^{-2}
NMSE_{Y_2}	2.3	1.3	10^{-2}

Table 2: NMSE obtained using the different methods for medium- and high-energy in-phase mode motions of the nonlinear nonconservative system.

5 Conclusions

In this paper, a new numerical method for the computation of NNMs of nonlinear mechanical structures is introduced. The approach targets the computation of undamped and damped invariant manifolds and solves the manifold-governing PDEs using the FE method. The use of the FE method renders the method general and systematic.

The method was demonstrated using linear and nonlinear two-DOF systems, both in conservative and non-conservative cases. Unlike the power series expansion method proposed by Shaw and Pierre, the FE-based method is not restricted to small-amplitude motions and has a convergence domain that is known *a priori*.

Acknowledgments

The authors would like to thank Prof. Ludovic Noels and Dr. Maxime Peeters for all the constructive discussions. The author L. Renson would like to acknowledge the Belgian National Fund for Scientific Research (FRIA fellowship) for its financial support.

References

[1] K. Worden, G.R. Tomlinson, *Nonlinearity in Structural Dynamics: Detection, Identification and Modelling*. Institute of Physics Publishing, Bristol and Philadelphia, 2001.

[2] G. Kerschen, K. Worden, A.F. Vakakis, J.C. Golinval, Past, present and future of nonlinear system identification in structural dynamics, *Mechanical Systems and Signal Processing* 20 (2006), 505-592.

[3] R.M. Rosenberg, Normal modes of nonlinear dual-mode systems, *Journal of Applied Mechanics* 27 (1960), 263-268.

[4] R.M. Rosenberg, On nonlinear vibrations of systems with many degrees of freedom, *Advances in Applied Mechanics* 9 (1966), 155-242.

[5] S.W. Shaw, C. Pierre, Non-linear normal modes and invariant manifolds, *Journal of Sound and Vibration* 150 (1991), 170-173.

[6] S.W. Shaw, C. Pierre, Normal modes for non-linear vibratory systems, *Journal of Sound and Vibration* 164 (1993), 85-124.

[7] L. Jezequel, C.H. Lamarque, Analysis of nonlinear dynamic systems by the normal form theory, *Journal of Sound and Vibration*, 149 (1991), 429-459.

[8] M.E. King, A.F. Vakakis, An energy-based formulation for computing nonlinear normal-modes in undamped continuous systems, *Journal of Vibration and Acoustics* 116 (1994), 332-340.

[9] A.F. Vakakis, L.I. Manevitch, Y.V. Mikhlin, V.N. Pilipchuk, A.A. Zevin, *Normal Modes and Localization in Nonlinear Systems*, John Wiley & Sons, New York, 1996.

[10] C. Touzé, O. Thomas, A. Huberdeau, Asymptotic non-linear normal modes for large-amplitude vibrations of continuous structures, *Computers & Structures* 82 (2004), 2671-2682.

[11] J.C. Slater, A numerical method for determining nonlinear normal modes, *Nonlinear Dynamics* 10 (1996), 19-30.

[12] Y.S. Lee, G. Kerschen, A.F. Vakakis, P.N. Panagopoulos, L.A. Bergman, D.M. McFarland, Complicated dynamics of a linear oscillator with a light, essentially nonlinear attachment, *Physica D* 204 (2005), 41-69.

[13] R. Arquier, S. Bellizzi, R. Bouc, B. Cochelin, Two methods for the computation of nonlinear modes of vibrating systems at large amplitudes, *Computers & Structures* 84 (2006), 1565-1576.

[14] F.X. Wang, A.K. Bajaj, Nonlinear normal modes in multi-mode models of an inertially coupled elastic structure, *Nonlinear Dynamics* 47 (2007), 25-47.

[15] M. Peeters, R. Vigui, G. Srandour, G. Kerschen, J.C. Golinval, Nonlinear normal modes, Part II: Toward a practical computation using numerical continuation, *Mechanical Systems and Signal Processing* 23 (2009), 195-216.

[16] M. Peeters, G. Kerschen, J.C. Golinval, C. Stephan, P. Lubrina, Nonlinear normal modes of real-world structures: application to a full-scale aircraft, *ASME International Design Engineering Technical Conferences*, Washington, USA (2011).

[17] E. Pesheck, Reduced-order modeling of nonlinear structural systems using nonlinear normal modes and invariant manifolds, *PhD Thesis*, University of Michigan, Ann Arbor, 2000.

[18] E. Pesheck, C. Pierre, S.W. Shaw, A new Galerkin-based approach for accurate non-linear normal modes through invariant manifolds, *Journal of Sound and Vibration* 249 (2002), 971-993.

[19] F. Blanc, K. Ege, C. Touzé, J.F. Mercier, A.S. Bonnet Ben Dhia, Sur le calcul numrique des modes non-linaires (On the numerical computation of nonlinear normal modes), *Congrs Francais de Mcanique*, Besancon, France, 2011.

[20] D. Noreland, S. Bellizzi, C. Vergez, R. Bouc, Nonlinear modes of clarinet-like music instruments, *Journal of Sound and Vibration* 324 (2009), 983-1002.

[21] D. Laxalde, F. Thouverez, Complex non-linear modal analysis for mechanical systems: Application to turbomachinery bladings with friction interfaces, *Journal of Sound and Vibration* 322 (2009), 1009-1025.

[22] G. Kerschen, M. Peeters, J.C. Golinval, A.F. Vakakis, Nonlinear normal modes, Part I: A useful framework for the structural dynamicist, *Mechanical Systems and Signal Processing* 23 (2009), 170-194.

[23] O.C. Zienkiewicz, R.L. Taylor, J.Z. Zhu, *The finite element method: Its basis and fundamentals*, Butterworth-Heinemann, Sixth edition, 2005.

[24] M. Renardy, R.C. Rogers *An introduction to Partial Differential Equations*, Springer-Verlag, 2004.

[25] P.B. Bochev, M.D. Gunzburger, *Least-Squares Finite Element Methods*, Springer, 2009.

[26] J.S. Hesthaven, T. Warburton, *Nodal Discontinuous Galerkin Methods: Algorithms, Analysis, and Applications*, Springer, 2008.